

Article

Responses of Tree Growth and Intrinsic Water Use Efficiency to Climate Factors and Human Activities in Upper Reaches of Tarim River in Alaer, Xinjiang, China

Yuanda Ye ^{1,2}, Yu Liu ^{1,3,4,5,6,*}, Meng Ren ^{1,7}, Qiufang Cai ^{1,3,4} , Changfeng Sun ^{1,5} , Qiang Li ^{1,5} , Huiming Song ^{1,5}, Mao Ye ⁸ and Tongwen Zhang ⁹ 

¹ State Key Laboratory of Loess and Quaternary Geology, Institute of Earth Environment, Chinese Academy of Sciences, Xi'an 710061, China

² University of Chinese Academy of Sciences, Beijing 100049, China

³ Center for Excellence in Quaternary Science and Global Change, Chinese Academy of Sciences, Xi'an 710061, China

⁴ Qingdao National Laboratory for Marine Science and Technology, Qingdao 266237, China

⁵ School of Human Settlements and Civil Engineering, Xi'an Jiaotong University, Xi'an 710049, China

⁶ China-Pakistan Joint Research Center on Earth Sciences, Chinese Academy of Sciences-Higher Education Commission, Islamabad 45320, Pakistan

⁷ Xi'an Institute for Innovative Earth Environment Research, Xi'an 710061, China

⁸ School of Geography Sciences and Touristy, Xinjiang Normal University, Urumqi 830054, China

⁹ Institute of Desert Meteorology, China Meteorological Administration, Urumqi 830002, China

* Correspondence: liuyu@loess.llqg.ac.cn

Abstract: With global warming and increasing human activities, exploring the impact of the rising atmospheric carbon dioxide concentration and climate change on forest ecosystems is crucial. In this study, we focus on Euphrates poplar (*Populus euphratica* Oliv.) in the upper reaches of the Tarim River in the Alaer region of Xinjiang. We use dendrochronological methods, tree-ring width, and stable carbon isotope series to explain basal area increment (BAI) and intrinsic water use efficiency (iWUE) changes. We further explore the influence of past climate change and human activities on the radial growth and iWUE of *P. euphratica* through stable oxygen isotope analysis combined with historical literature records. The results showed that relative humidity had an essential effect on $\Delta^{13}\text{C}$ and $\delta^{18}\text{O}$ fractionation in *P. euphratica* tree rings, whereas the vapor pressure deficit (VPD) was considered the main factor influencing the inter-annual variability of the iWUE and BAI. Since 1850, long-term variations in iWUE have exhibited an upward trajectory correlated with rising atmospheric CO₂ levels. Approximately 13% of this iWUE increase can be attributed to changes in carbon-concentration-induced water use efficiency (cc*i*WUE). Although $\Delta^{13}\text{C}$ and $\delta^{18}\text{O}$ were generally uncorrelated between 1850 and 2018, around 1918, their relationship changed from being weakly correlated to being significantly negatively correlated, which may record changes related to the upstream Tarim River diversion. During the period from 1850 to 2018, both the BAI and iWUE showed an increasing trend for *P. euphratica* growth; however, the relationship between them was not stable: during 1850–1958, both variables were mainly influenced by climatic factors, while during 1959–2018, the most important influence was due to human activities, specifically agricultural development and irrigation diversions. An abrupt surge in the BAI was observed from 1959 to 1982, reaching its peak around 1982. Surprisingly, post-1983, the escalating iWUE did not correspond with a continuation of this upward trajectory in the BAI, highlighting a divergence from the previous trend where the enhanced iWUE no longer facilitated the growth of *P. euphratica*. Despite *P. euphratica* having adapted to the continuously rising C_a, improving its iWUE and growth capacity, this adaptive ability is unstable and may easily be affected by human activities. Overall, the increase in C_a has increased the iWUE of *P. euphratica* and promoted its growth at a low frequency, while human activities have promoted its development at a high frequency.



Citation: Ye, Y.; Liu, Y.; Ren, M.; Cai, Q.; Sun, C.; Li, Q.; Song, H.; Ye, M.; Zhang, T. Responses of Tree Growth and Intrinsic Water Use Efficiency to Climate Factors and Human Activities in Upper Reaches of Tarim River in Alaer, Xinjiang, China. *Forests* **2023**, *14*, 1873. <https://doi.org/10.3390/f14091873>

Academic Editor: Matthew Therrell

Received: 18 August 2023

Revised: 8 September 2023

Accepted: 12 September 2023

Published: 14 September 2023



Copyright: © 2023 by the authors. Licensee MDPI, Basel, Switzerland. This article is an open access article distributed under the terms and conditions of the Creative Commons Attribution (CC BY) license (<https://creativecommons.org/licenses/by/4.0/>).

Keywords: stable isotopes; intrinsic water use efficiency; *Populus euphratica*; Tarim River Basin

1. Introduction

Forests play a crucial role in terrestrial ecosystems' carbon and water cycles, making it essential to understand how they respond to global change [1,2]. Human-induced CO₂ emissions over the past century have led to global warming and directly impacted land plants, significantly affecting their physiological and ecological processes [3–5]. Tree rings offer reliable information on age and environmental conditions due to their strong continuity and high resolution [6], as well as unequivocal traces of natural and anthropogenic disturbances [7]. By examining changes in tree rings, variations in environmental conditions can be inferred, allowing for an assessment of their impact on ecosystems [8]. Climate change affects tree rings' width and isotopic composition during growth. Carbon discrimination provides valuable information reflecting the ratio of internal leaf CO₂ (C_i) to ambient atmospheric CO₂ (C_a), along with intrinsic water use efficiency (iWUE) [9].

Meanwhile, the δ¹⁸O value of tree rings is mainly influenced by the δ¹⁸O source water and the enrichment of leaf water through evaporation [10], and, combined with δ¹³C, can reveal dynamic changes in the stomatal conductance and photosynthetic rate over time [11,12]. Changes in the iWUE may affect tree growth. When the iWUE increases, trees can assimilate more carbon per unit of water lost through transpiration, influenced by factors such as stomatal behavior and the vapor pressure deficit. However, the relationship between an increased iWUE and tree growth is complex, and influenced by various factors such as climate variability and plant functional types [13]. Some studies suggest that increasing iWUE does indeed promote tree growth [14–16], while others find that it does not necessarily lead to increased growth rates [17–19] because other limiting factors also affect tree growth, such as fertilization effects [20] or negative impacts from droughts that cannot be offset by an increased iWUE alone [21]. Sudden increases in iWUE may even serve as an early alert signal of an upcoming drought-induced mortality event [22].

Forests are under threat from various human activities. Over the past few decades, there has been a significant impact on the change in vegetation cover due to human activity [23]. Climate change caused by human activities can positively or negatively affect trees. While it may enhance hydrological cycles, it can also reduce rainfall during dry seasons [24]. Human actions at forest edges have altered microclimates, affecting tree growth in those areas [25]. Air pollution is another primary concern that significantly changes plant nutrition and soil chemical properties by depositing pollutants such as sulfur and nitrogen [26–30], leading to a potential forest decline. Unsustainable practices like land reclamation, road expansion, runoff regulation, and water diversion irrigation can negatively affect tree growth [31,32].

The Tarim River Basin is important in northwest China, where *P. euphratica* is a typical tree species. Desert riparian forests are major biomass generators in the inland river systems of arid regions and are well-adapted to long-term environmental conditions within these basins, making them an essential component of arid ecosystems. These forests have unique water-use strategies for survival, making them a hot topic among domestic and international ecologists. Researchers have studied stable isotopes tracing sources of *P. euphratica*'s water supply since the 1950s [33]. They have also studied ecological effects after artificial watering [34–36], and the relationship between the radial increment rate and groundwater level changes [34,37]. However, there has been little research on the comprehensive impacts of climate change or increases in atmospheric CO₂ concentrations, iWUE, or δ¹³C for *P. euphratica* [38].

The Alaer region upstream from the Tarim River Basin holds excellent potential for using tree rings to study responses to paleoclimates and human activities' environmental impact since agricultural development began in the 1950s, creating new oasis farmland amidst Gobi Desert wildernesses [39]. There has been no report regarding iWUE changes in the study area and its potential impact on tree growth. Therefore, this study focuses on *P. euphratica* in the Alaer area upstream from the Tarim River drainage to establish tree-ring width sequences, δ¹³C sequences, δ¹⁸O sequences, and iWUE sequences. The aim was to analyze how the increasing atmospheric carbon dioxide concentration (C_a) and human

activities affect the BAI and iWUE of *P. euphratica* by comparing historical BAIs with those of $\delta^{13}\text{C}$, $\delta^{18}\text{O}$, and the iWUE of *P. euphratica*. Examining the intrinsic water use efficiency of *P. euphratica* can help us to understand the water-use strategy of desert riparian forests, as well as provide data and theoretical support for their conservation.

2. Materials and Methods

2.1. Study Area and Sampling Location

Located on the south bank of the upper alluvial plain of the Tarim River (longitude $80^{\circ}30'–81^{\circ}58'$ E; latitude $40^{\circ}22'–40^{\circ}57'$ N), the sampling site is situated at the northwest edge of the Taklamakan Desert and the eastern end of the Tarim Reclamation Area of the First Agricultural Division. The altitude at this location is 1012 m (Figure 1). This area belongs to a typical temperate continental arid climate zone with little rainfall. The Tarim River is this region's primary irrigation water source, mainly supplied by glaciers and snow accumulation. The groundwater flows from west to east, consistent with the Tarim River's direction. The vegetation primarily consists of shrubs, grassland, and alpine forests dominated by *P. euphratica*, while the soil types are predominantly desert brown soils and saline soils. According to the International Tree Ring Data Bank's sampling criteria, samples were collected from 25 living trees. Each tree was cored twice in different directions using a 5 mm internal diameter borer. This group of samples is referred to as the ALE.

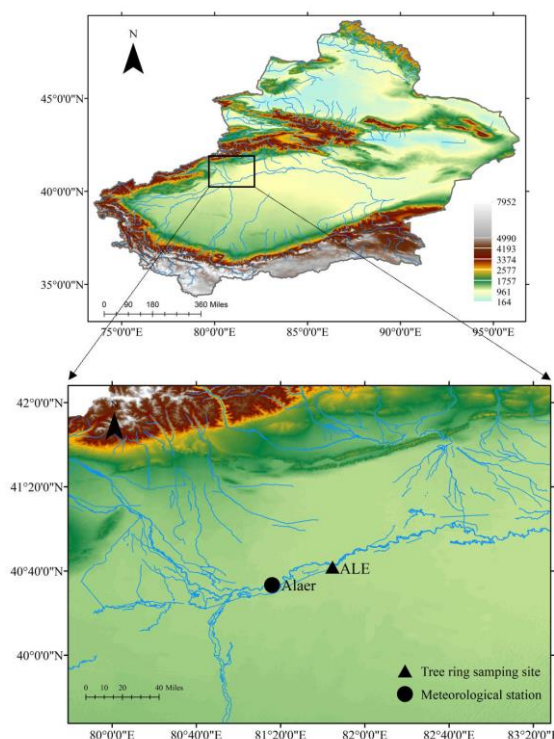


Figure 1. Tree-ring sampling sites and map of meteorological stations in Alaer, Xinjiang, China.

2.2. Tree Ring Analysis

During sampling, healthy and older trees were selected. The collected cores were returned to the laboratory, where they were dried and sanded until the annual rings became visible. LINTAB 6 was used to measure the core widths with an approximate precision of 0.01 mm, followed by cross-dating using TSAPwin software version 4.81 (Rinnotech, Heidelberg, Germany) and verification with the COFECHA program for accuracy [40]. The resulting ring-width series were detrended and normalized into a chronology with Mod Neg Exp in the “dplR” package in R language [41].

For analysis purposes, we converted the ring width into the basal area increment (BAI) while minimizing errors by selecting fifteen trees with piths over one hundred years

old for BAI calculation; individual BAI values were calculated before averaging them into a regional BAI sequence. Based on our research objectives and the length of stable carbon isotope sequences in tree rings, we chose the period between 1850 and 2018 as our study period. The BAI was calculated by assuming that the cross-section of a tree trunk is circular and converting the width values of each annual ring into the corresponding BAI values. The formula for the basal area increment is as follows: $BAI = \pi(r_t^2 - r_{t-1}^2)$, where r_t represents the growth radius of the basal section in year t , r_{t-1} represents the growth radius of the basal section in year $t - 1$, and BAI represents the basal area increment in year t . The BAI was calculated using the “R” language [42], utilizing the “bai.out” command for computation.

2.3. The $\delta^{13}\text{C}$ and $\delta^{18}\text{O}$ Analyses

Based on accurate dating, four samples (ALE-03A, ALE-15A, ALE-26B, and ALE-54B) with clear tree rings, no fractures, and no contamination were selected for stable isotope measurement. Each annual ring was separated with a fine and sharp knife under a microscope. To reduce variation in the isotope signatures, we used the extracted alfa-cellulose in this study [43]. The oxygen isotope ratios were measured using a Delta V Advantage mass spectrometer coupled with a high-temperature pyrolysis elemental analyzer (TC/EA). Fibrous cellulose samples weighing 0.12–0.16 mg were placed in silver cups, with every eight samples inserted into one standard sample. An autosampler automatically pushed each packaged sample into the high-temperature pyrolysis elemental analyzer. We selected MERCK cellulose microcrystalline (27.7‰) as our laboratory standard [44]. The $\delta^{18}\text{O}$ value represents the oxygen isotope ratio of the measured sample relative to the Vienna Standard Mean Ocean Water (VSMOW) standard sample, with an analytical precision of less than $\pm 0.2\text{\textperthousand}$ after correction against Merck sample $\delta^{18}\text{O}$ values. The FLASH2000 elemental analyzer combined with the Delta V Advantage isotope mass spectrometer was used to measure the $\delta^{13}\text{C}$ value of the samples by burning them in an element analyzer and transferring the CO_2 produced during combustion to a mass spectrometer through a CONFLO IV continuous flow interface. Carbon isotope ratios were presented as deviations relative to Pee Dee Belemnite (PDB), and according to repeated measurements based on working standards, their accuracy was less than $\pm 0.2\text{\textperthousand}$. Finally, the calibrated tree-ring $\delta^{13}\text{C}$ actual values were obtained by correcting the measured tree-ring $\delta^{13}\text{C}$ values against IAEA-CH-3 [45] values.

2.4. Calculation of Physiological Parameters

We assumed the Farquhar et al. [9] theory to correlate the carbon discrimination and the internal and atmospheric CO_2 partial pressure. The carbon isotope discrimination in C_3 plants can be represented as follows.

$$\Delta^{13}\text{C} = (\delta^{13}\text{C}_{\text{atm}} - \delta^{13}\text{C}_{\text{tree}})/(1 + \delta^{13}\text{C}_{\text{tree}}/1000) \quad (1)$$

where $\delta^{13}\text{C}_{\text{atm}}$ is the $\delta^{13}\text{C}$ value of atmospheric CO_2 and $\delta^{13}\text{C}_{\text{tree}}$ is the $\delta^{13}\text{C}$ value of tree-ring cellulose.

$\Delta^{13}\text{C}$ values can also be calculated as the following equation [10]:

$$\Delta^{13}\text{C} = a + (b - a)(C_i/C_a) \quad (2)$$

where a ($\sim 4.4\text{\textperthousand}$) represents the isotopic discrimination that results from the diffusion of CO_2 from the atmosphere into the intercellular space of cells, b ($\sim 27\text{\textperthousand}$) represents the isotopic discrimination caused by the discrimination of RuBP carboxylase against $^{13}\text{CO}_2$ [10], and C_i and C_a represent the concentration of CO_2 in the leaf intercellular spaces and the atmosphere, respectively.

The intrinsic water use efficiency is specified as the ratio of the carbon assimilation rate (A) to the stomatal conductance (g_s) [46]. The calculation formula is as follows:

$$iWUE = A/g_s = C_a \times [(1 - C_i/C_a)/1.6] \quad (3)$$

To remove the impact of climate signals on water use efficiency, it is necessary to first separate the climate signal from the atmospheric CO₂ concentrations inside the leaves [47]. Specifically, the initial step involves correlating C_i with monthly climate variables to identify the month with the most significant correlation. Subsequently, principal component analysis is performed on climate factors such as temperature, precipitation, and vapor pressure deficit (VPD) to obtain the optimum climatic target (PCT). Then, by using the empirical formula $C_i + \tau \times (C_a - 280)$ and changing the τ values ($\tau \in [-1, 2]$, step length 0.004), a series of simulated intra-leaf CO₂ concentration sequences (C_i -climate) can be obtained [47]. The pre-industrial atmospheric CO₂ concentration, used as a baseline in this study, was approximately 280 ppm, adopted by the Intergovernmental Panel on Climate Change (IPCC) as the pre-industrial baseline for CO₂ [48]. When the variance explained via the simulated C_i -climate sequence is highest for the PCT and their residual sequence has the slightest slope, this simulation sequence is considered optimal; it represents changes in intra-leaf CO₂ concentrations caused by climatic factors. The difference between them represents changes in water use efficiency caused by an increased CO₂ concentration. Finally, ^{cc}iWUE can be obtained through the formula $C_i + \tau \times (C_a - 280)$.

2.5. Climate Data

The sampling point is located near the Alaer Meteorological Station (40°33' N, 81°16' N) at 1012 m. The annual total precipitation at the Alaer Station during 1959–2018 (Figure 2) was 505.67 mm, with rainfall mainly concentrated in the months of June to August. The region experiences high evaporation rates, averaging 2110.50 mm per year. The hottest month is July, with an average temperature of 24.80 °C, while January is the coldest month, with an average temperature of −8.28 °C and an annual average temperature of 10.79 °C. The relative humidity averages 53.29% annually, with April being the driest month, recording a humidity level of 36.48%, and December being the most humid month, recording a humidity level of 69.04%. Climate data were downloaded from the Meteorological Information Center of China (<http://data.cma.cn/>, accessed on 10 April 2021).

The vapor pressure deficit (VPD) reflects the air water potential, influencing plant stomatal closure, thereby controlling physiological processes such as transpiration and photosynthesis that significantly affect crop water loss through transpiration and evaporation. The value can be calculated using the relative humidity (RH) and temperature (T) using this formula:

$$VPD = (1 - RH) \times 0.6108 \times e^{(17.27T/(T + 273.3))} \quad (4)$$

VPD represents the monthly mean vapor pressure deficit, RH is the monthly mean relative humidity, and T is the monthly mean temperature.

2.6. Data Analysis

Traditional mathematical and statistical methods were utilized in dendroclimatology to analyze the data. The Pearson correlation coefficient (r) was calculated to investigate the relationship between the measured climate data and various tree-ring width indices, including the BAI, and stable isotope series such as Δ¹³C and δ¹⁸O, and C_i and iWUE. Furthermore, a 31-year sliding correlation was conducted to investigate temporal trends in the relationships between tree-ring Δ¹³C and δ¹⁸O, BAI, and iWUE. The relevance, linear regression, and time series analysis were performed using the SPSS 25.0 statistical software package (SPSS, Chicago, IL, USA).

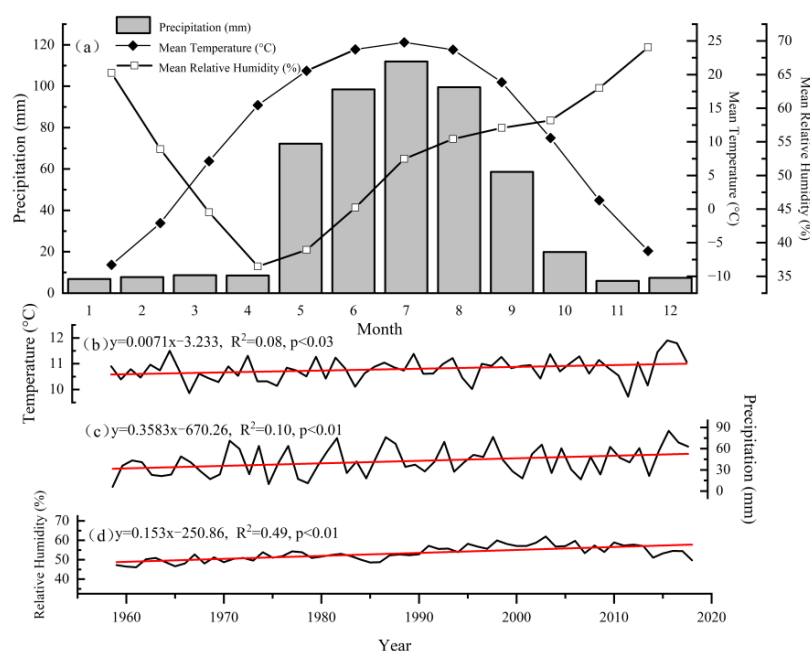


Figure 2. The intra-annual (a) and annual variations (b–d) of temperature, precipitation, and relative humidity of the Alaer Meteorological Station (red lines represent the linear regression lines).

3. Results

3.1. The Trends of Tree-Ring Width, Tree-Ring Width Index, and BAI

Starting in 1958, humans began cultivating the Alaer area [39], dividing its history into 1850–1958 and 1959–2018. Our findings indicate that from 1850 to 2018, tree-ring width exhibited an upward trend. After a rapid increase post-1958, tree-ring width showed a downward trend after 1977 (Figure 3a). Figure 3b illustrates that the index of tree-ring width reached its maximum value in 1982, with relatively high growth periods between 1865–1894 and 1960–1994, when the tree-ring width steadily increased above average values. From 1904 to 1957 was a period of relatively low growth, while fluctuations decreased after 1994. The BAI continued to grow from 1850 to 2018, with an average value of $19.78 \text{ cm}^2/\text{year}$, reaching its peak in 1982. From 1962 to 2018, the BAI and tree-ring width displayed similar changes (Figure 3c), indicating that human influence led to rapid growth followed by slower increases.

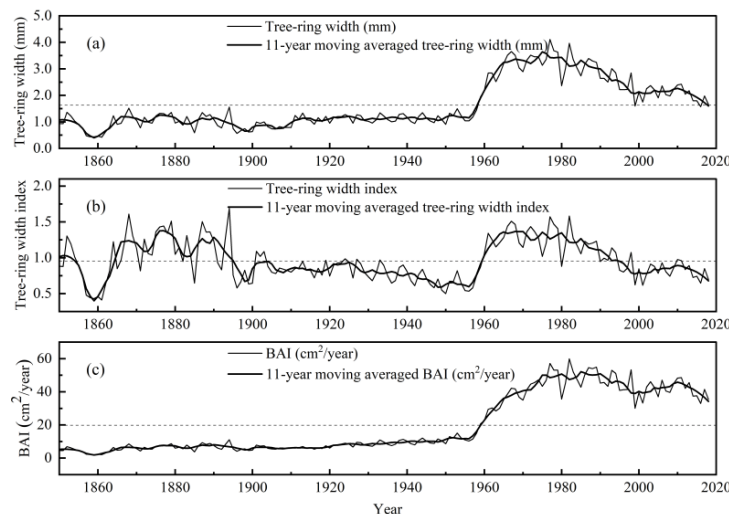


Figure 3. Trends of (a) tree growth, (b) the standard ring-width index, and (c) the basal area index (BAI) from 1850 to 2018. Dashed lines represent the average values.

3.2. Long-Term Changes in $\Delta^{13}\text{C}$ and $\delta^{18}\text{O}$, and iWUE and $\delta^{18}\text{O}$

Between 1850 and 2018, the correlation between the $\Delta^{13}\text{C}$ and $\delta^{18}\text{O}$ in tree rings from *P. euphratica* was weak overall. However, around 1918, this relationship changed in intensity and direction, becoming significantly negatively correlated ($r = -0.52, p < 0.01$ in Figure 4b). The moving correlation analysis over 31 years suggests that factors controlling the $\Delta^{13}\text{C}$ and $\delta^{18}\text{O}$ have changed. From 1918 to 2018, there was a significant correlation between $\delta^{18}\text{O}$ and iWUE ($r = 0.25, p < 0.01$ in Figure 4d), with changes in the $\delta^{18}\text{O}$ explaining up to 6% of the variation in the iWUE.

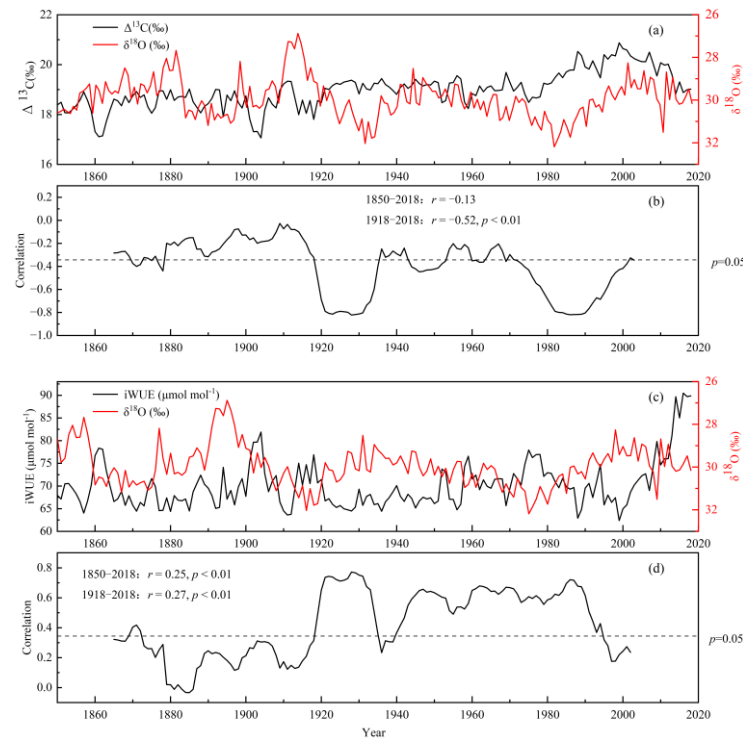


Figure 4. Comparisons and correlations of $\Delta^{13}\text{C}$ and $\delta^{18}\text{O}$ of *P. euphratica* during 1850–2018. (a) $\Delta^{13}\text{C}$ and $\delta^{18}\text{O}$, (c) iWUE and $\delta^{18}\text{O}$, and (b,d) the 31-year sliding correlations of both isotopes of *P. euphratica*. The dashed lines represented the confidence of $p = 0.05$.

3.3. Climate Response of $\Delta^{13}\text{C}$, $\delta^{18}\text{O}$, C_i , BAI, and iWUE

The climate monitoring data from 1958 to 2018 indicate that the average annual temperature in the Alaer region remained relatively stable, while the average yearly precipitation presented a remarkable increasing tendency, with a growth rate of 0.35 mm/a. Additionally, the relative humidity exhibited a notable increasing trend, with a growth rate of 0.15 mm/a (Figure 2). The Pearson correlation analysis determined the relationship between the Alaer tree-ring $\Delta^{13}\text{C}$ chronology and various climatic factors. The results indicated (Figure 5a) a significant correlation between stable carbon isotope series of *P. euphratica* tree rings in Alaer and the mean temperature and relative humidity during the growing season (April–September). Negative correlations were observed with the monthly average temperature from July to September, while positive correlations were found with the monthly average relative humidity from April to September. The tree-ring $\delta^{13}\text{C}$ was positively correlated with growing season precipitation and relative humidity, suggesting that water vapor pressure changes were the main factors determining $\delta^{13}\text{C}$ fractionation during this period. In contrast, the tree-ring $\delta^{18}\text{O}$ had an opposite response direction under the influence of temperature and moisture conditions (precipitation and relative humidity) (Figure 5b). April through September are the months exerting the most significant impact on tree-ring $\delta^{18}\text{O}$. VPD and relative humidity displayed the most robust correlations during this period, with $r = 0.61, p < 0.01$ and $r = -0.66, p < 0.01$, respectively.

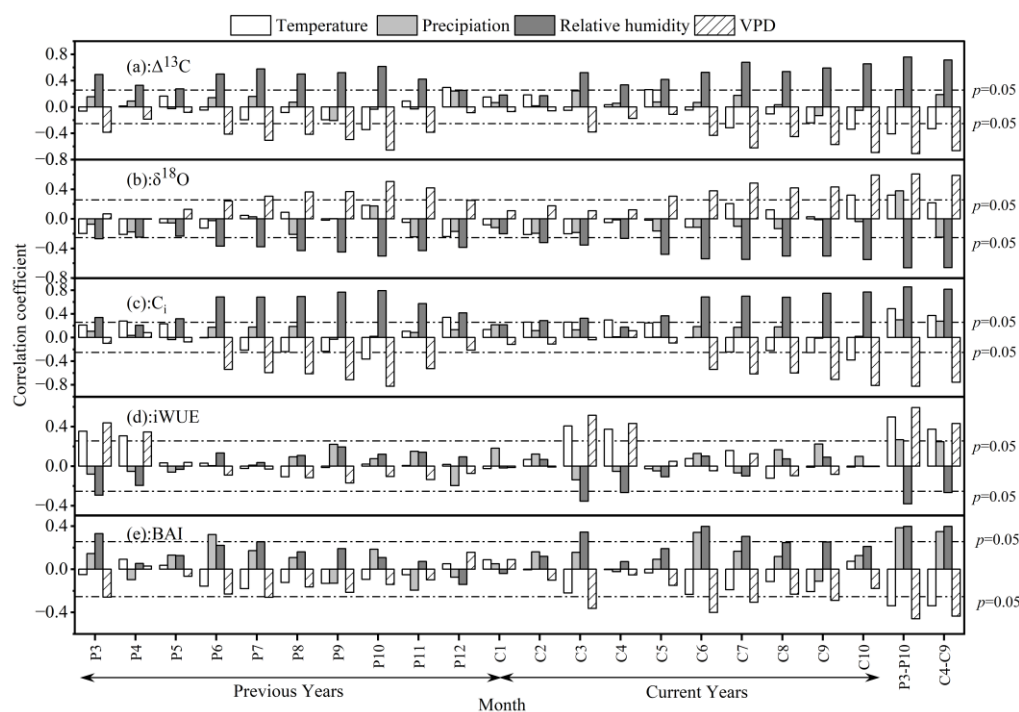


Figure 5. Correlational analysis between tree-ring $\Delta^{13}\text{C}$, $\delta^{18}\text{O}$, C_i , iWUE, BAI, and climate variables to examine monthly combinations from 1959 to 2018.

The correlation analysis also revealed that the C_i was positively correlated with the early stages of the growing season as well as temperatures in April–May ($r = 0.37, p < 0.05$); however, its relationship with precipitation was weak overall but stronger when considering May through September's mean relative humidity ($r = 0.81, p < 0.05$). The C_i had negative correlations, mainly concentrated on May through September ($r = -0.76, p < 0.01$), with a VPD throughout most months. The response between the mean relative humidity from May to September and the C_i had the best correlation coefficient ($r = 0.81, p < 0.05$ Figure 5c). In the early growing season, the iWUE is more sensitive to the temperature and VPD in March and April, with correlation coefficients of 0.50 and 0.59, respectively (Figure 5d), while its relationship with precipitation was weak overall but most vital when considering the VPD from March to April in a year. Finally, the BAI was negatively correlated with temperature from May to September, during which the BAI responded significantly positively to the precipitation ($r = 0.35, p < 0.01$) and relative humidity in June ($r = 0.4, p < 0.01$). The highest correlation between the VPD from May through July and the BAI reached -0.43 ($p < 0.05$, Figure 5e).

3.4. Long-Term Changes of C_i and iWUE

Using meteorological data from Alaer between 1959 and 2018, we conducted a principal component analysis on the temperature, precipitation, relative humidity, and VPD. The first principal component explained 78.85% of the total variance and was used as the target climate factor (PCT) to calculate the C_i -climate. We found that the correlation between the C_i -climate at $\tau = 0.175$ and the PCT was the highest ($r = 0.89, p < 0.01$, in Figure 6c), with their residual slope reaching a minimum.

Between 1850 and 2018, the C_a increased by approximately 122 ppmv, while the C_i gradually rose from 1850, with a maximum value exceeding 273.36 ppmv (Figure 6a). Compared to the mean C_i value from 1850 to 1859, the last decade (2009–2018) saw an increase of only 111.44 ppmv in C_a , while a rise of 87.27 ppm occurred in C_i , thus indicating that the magnitude of the increase in C_i is lower than that of C_a .

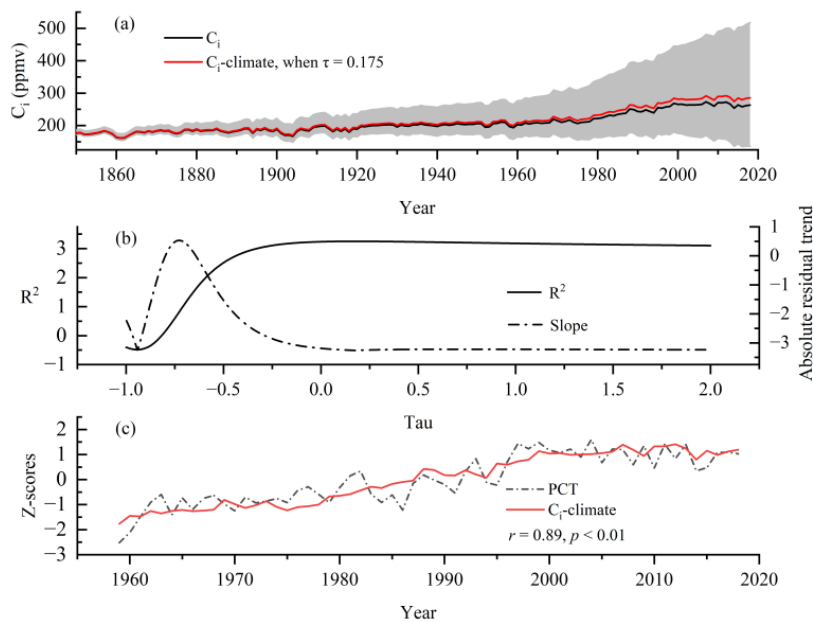


Figure 6. (a): Tree rings' estimated C_i and the intercellular CO_2 concentration series (C_i -climate), which was calculated using the empirical equation; (b): the grey area indicates all calculated C_i -climate time series when changing τ from -1 to 2 ; (c): C_i -climate explains the variance in instrumental target (PCT) and changes in the absolute residual trend; comparison between C_i -climate and PCT.

The sequence of the changes in C_i influenced by climate factors (C_i -climate at $\tau = 0.175$) had the highest explanatory variance for C_i at 78.85% (Figure 6c). Looking at their rate of change, the C_i and C_i -climate had average values of 12.72% and 14.53%, respectively. The difference between them mainly occurred after 1950 (Figure 7a).

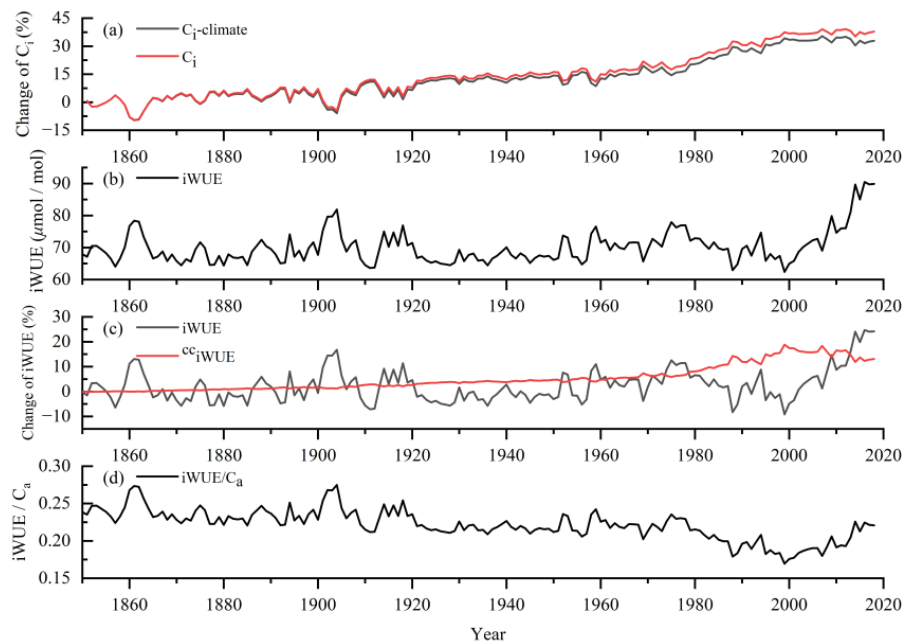


Figure 7. The variation of C_i (a) and iWUE (b), and percent change in iWUE (c) and $i\text{WUE}/C_a$ (d) from 1850 to 2018.

There is an increasing trend in iWUE in the Alaer region, especially after 2000, with an average value of $77.60 \mu\text{mol/mol}$ compared to $69.50 \mu\text{mol/mol}$ from 1850 to 1859, indicating an increase of $8.10 \mu\text{mol/mol}$ or approximately 10% (Figure 7b). As shown in

Figure 7c, the water use efficiency caused by the carbon dioxide concentration (cc iWUE) also exhibits an upward trend, with a growth rate of 13%. Further, the change in iWUE from 1850 to 2018 was closer to the predicted value under a constant C_i/C_a scenario [49], explaining 10.30% of the variation in the iWUE and indicating that trees have become more responsive to CO_2 increase. Additionally, we calculated the rate of change in iWUE relative to C_a , denoted as (iWUE/C_a) . From 1850 to 2018, the average growth rate of the iWUE relative to the C_a was 0.22, and all growth rates were positive (Figure 7d). When we divided the data into before and after 1965 (commonly used as a reference point for the rapid increase in C_a [50]), the average iWUE/C_a from 1901 to 1965 was 0.23, while it was 0.20 from 1966 to 2018, a decrease of about 13%.

3.5. Relationship between BAI and iWUE of *Populus euphratica*

The iWUE of tree rings is negatively associated with the $\Delta^{13}\text{C}$ of tree rings ($r = -0.32$, $p < 0.01$), indicating that the photosynthetic rate contributes to the variation in iWUE. However, the iWUE positively correlates with the $\delta^{18}\text{O}$ of tree rings ($r = 0.24$, $p < 0.01$), indicating that stomatal conductance also contributes to the variation in iWUE. During 1959–2018, there was no significant relationship between the iWUE and the $\delta^{18}\text{O}$, suggesting that other factors may have influenced the changes in iWUE over this period.

Over the past 160 years, the iWUE and BAI of *P. euphratica* in the upper Tarim River have generally increased, correlating positively ($r = 0.32$, $p < 0.01$, $n = 169$). This correlation fluctuates, with negative phases after 2012, 1867–1872, and 1914–1929, and positive phases during 1878–1898, 1941–1957, and 1969–1974. No significance was found in other periods. Since the late 1980s, the correlation between the iWUE and BAI has attenuated. The first-order difference analysis indicated no significant correlation between the high-frequency BAI and iWUE. Thus, iWUE has a direct relationship with radial growth over long-term changes, but their correlation is not strong Figure 8.

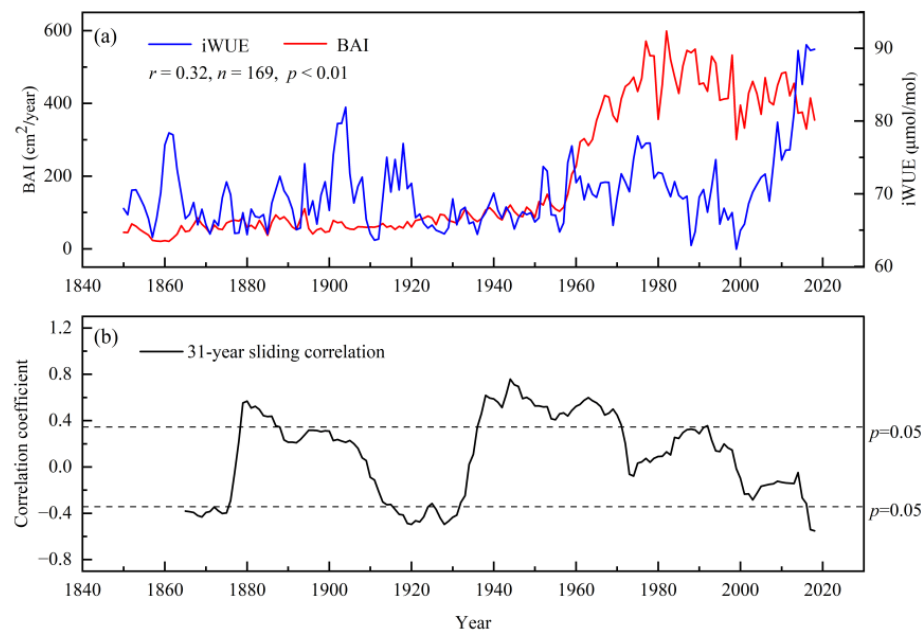


Figure 8. Comparison of tree BAI and iWUE from 1850 to 2018 (a), yearly values, and (b) the 31-year sliding correlation. Dashed lines represent the range of the confidence intervals.

4. Discussion

4.1. The Impact of Climate and Human Activities on the Growth Process

The desert riparian forest is the primary vegetation type in arid inland river basins. Its growth and development are mainly influenced by soil moisture and groundwater depth. However, due to the dry climate, limited precipitation, intense evaporation, and

extremely scarce water resources in these basins, desert riparian forests' distribution, survival, and succession are severely restricted [51]. The core issue of plant drought resistance and water-saving mechanisms is the regulation of water relations. Stomata are channels for leaf transpiration and for photosynthetic CO₂ to enter cells. The ability of plants to regulate stomatal opening enables them to adjust their transpiration rate. A high gradient or differential in the VPD between inside and outside leaves causes a decrease in stomatal conductance for most plants, resulting in reduced transpiration consumption [52]. Most plants decrease their stomatal conductance under elevated VPD conditions, which typically leads to reduced transpiration, photosynthesis, and, potentially, radial growth, as an adaptive strategy to meet their water balance requirements [53]. The BAI is markedly negatively related to the temperature and VPD from May to September. The correlation coefficient between the BAI and the VPD from May to July reaches -0.43 ($p < 0.01$, $n = 51$; Figure 5). Meanwhile, the BAI has a significant forward correlation to precipitation and relative humidity in the growing season. These correlations suggest that water stress is the leading environmental factor affecting tree radial growth, especially during the growing season. The high summer temperatures exceeded the suitable levels for photosynthesis. At the same time, the shallow groundwater depth did not limit stomatal conductance(g_s), thus increasing the internal carbon dioxide concentration (C_i) within leaves, leading to the negative correlation between the BAI and the VPD under these two factors' combined effect.

There is a negative correlation between the carbon isotopes ($\Delta^{13}\text{C}$) and oxygen isotope ratios ($\delta^{18}\text{O}$) in tree rings [38]. Tree-ring $\delta^{13}\text{C}$ reflects changes in the C_i/C_a , while tree-ring $\delta^{18}\text{O}$ mainly reflects changes in the relative humidity. The relationship between the $\delta^{13}\text{C}$ and $\delta^{18}\text{O}$ can be used to deduce changes in plants' intrinsic water use efficiency. Changes in both the photosynthetic rate (A) and stomatal conductance (g_s) can cause variations in tree-ring $\delta^{13}\text{C}$ [11], whereas only stomatal conductance affects tree-ring $\delta^{18}\text{O}$ [54]. If the change in the photosynthesis rate is more significant than that of the stomatal conductance, there will be no correlation between the values of the $\delta^{18}\text{O}$ and the $\delta^{13}\text{C}$; if A increases but g_s remains unchanged, then there will be a negative correlation between the values of the $\delta^{13}\text{C}$ and the $\delta^{18}\text{O}$ [11,12]. From 1850 to 2018, the $\Delta^{13}\text{C}$ and $\delta^{18}\text{O}$ were generally unrelated; however, around 1918, this relationship changed from being irrelevant to being significantly negatively correlated. This result suggests that factors controlling the $\Delta^{13}\text{C}$ and $\delta^{18}\text{O}$ may have changed during this period. Based on field investigations, historical documents, and maps, Han Chunxian [55] researched the Shaya section of the mainstream Tarim River above and below Alaer (located upstream of Shaya). The analysis showed that in the 1910s, the Shaya section shifted northward along its upstream river course, following a position along the northern river. According to historical records and deductions based on $\Delta^{13}\text{C}$ - $\delta^{18}\text{O}$ relationships, there may have been a channel shift in the upstream reaches of the Tarim River around 1918.

Since large-scale agricultural development began in the 1950s, human activities have increasingly altered natural water–sediment processes within the Tarim River Basin [56], leading to significant changes in the river's geomorphology. In addition, groundwater has been extensively used for irrigation along the Tarim River basin, leading to increased groundwater levels [57]. According to previous studies on land reclamation, before its development, the underground water depth was 5–7 m [39]; after the construction of irrigation systems, it rose by about 1–4 m [58]. Peng et al. [59] showed that desert poplars rely heavily on groundwater for growth, with the groundwater level being the foremost environmental element influencing radial growth. Groundwater depth directly affects soil moisture dynamics [60] and nutrient dynamics [61], which are the main factors determining *P. euphratica*'s distribution, development, and population succession [34,62,63]. In arid environments with strong evaporation rates, high groundwater levels can lead to ineffective dissipation due to evaporation and cause soil salinization that stresses plants; low groundwater levels can inhibit plant growth due to water stress leading to the degradation or even death of vegetation, resulting in desertification [64]. Wang Jing [65] employed a geographic detector to conduct a simulation analysis exploring the relationships between artificial

and natural oasis vegetation in Alaer, as well as various soil and groundwater elements. The study revealed that mineralization was the primary determinant affecting vegetation distribution and growth among the factors influenced by groundwater. Hou et al. [66] believed that soil salinization is a major factor inhibiting the growth of *P. euphratica* forests, with reducing salt content in soils being a priority measure for ecological restoration.

The above analysis shows that the incremental growth of *P. euphratica* was influenced by various climate and environmental factors. Although the impact of climate factors on its radial growth is relatively low, human activities such as agricultural development and irrigation have led to a reduction in the Tarim River's flow, changes in groundwater depth, soil salinization, and other problems, which have had a profound impact on the radial growth of Alaer *P. euphratica*.

4.2. Analysis of the Reasons for Changes in Intrinsic Water Use Efficiency of *Populus Euphratica* and Its Relationship with BAI

Under elevated levels of CO₂, plant stomata tend to close, reducing water loss and potentially improving intrinsic water-use efficiency (iWUE). The effect on photosynthesis and intercellular CO₂ concentration can vary depending on other environmental factors [67]. This study found that C_a significantly increased, resulting in a 13% change in water use efficiency (^{cc}iWUE) (Figure 7), indicating that the increase in atmospheric carbon dioxide has a particular promoting effect on the iWUE. In addition, the iWUE changes from 1850 to 2018 are closer to the predicted values under the constant C_i/C_a scenarios [49], explaining 10.3% of the iWUE changes and suggesting that trees are becoming more responsive to increases in CO₂. The observed 13% increase in iWUE is comparatively modest when set against non-riparian species [68]. Climate factors such as temperature, precipitation, relative humidity, and vapor pressure deficit can also affect plants' stomatal conductance and photosynthetic rates, and further influence iWUE. Research has demonstrated that desert plants resist drought stress by increasing their water use efficiency. When *P. euphratica* experiences moderate drought stress, the stomatal aperture decreases to reduce water loss while increasing intrinsic water use efficiency [69]. The core issue of plants' drought resistance mechanisms is the regulation of water relations through stomata channels, where leaf transpiration occurs and photosynthetic raw materials enter cells; therefore, regulating stomatal opening allows plants to adjust their transpiration rates. An increase in the VPD causes most plant leaf stomatal conductance to decrease while reducing transpiration consumption [52] to adapt to moisture balance and survival needs. Accordingly, our correlation analysis results show that iWUE significantly correlates with VPD during most months. A larger VPD indicates less atmospheric moisture because when VPD values are high, plants have more substantial pressure to lose water, causing them to close their stomata, thereby reducing intercellular CO₂ concentration and plant photosynthesis. Zhang et al. [70] suggested that the increase in VPDs caused by global warming may be a reason for the annual growth of 0.13% in ecosystems' iWUEs. Therefore, rising greenhouse temperatures and increasing values of VPD could result in more intense droughts, potentially affecting plant and forest ecosystems [71]. They indicated that VPD has an essential impact on iWUE in the Alaer region.

Over the past 160 years, iWUE has shown a clear growth trend in the *P. euphratica* growing upstream of the Tarim River. However, since the late 1990s, with increased human activities, this correlation has weakened due to the increased relative humidity (Figure 2d), which reduces stomatal conductance and thus decreases iWUE. The dependence on climate δ¹⁸O signals can explain whether changes in the iWUE were caused by differences in stomatal conductance or changes in the photosynthetic rate [38]. Tree-ring δ¹⁸O is positively correlated with iWUE ($r = 0.24, p < 0.01$), indicating that stomatal conductance also contributes to the variation of iWUE. In contrast, the transition from no correlation between tree-ring Δ¹³C and δ¹⁸O to a significant negative correlation (Figure 4c) after 1918 critically suggests the increase in stomatal conductance in determining tree-ring Δ¹³C, thus highlighting its essential contribution to regulating iWUE. The changing impact of

stomatal conductance on variations in iWUE is revealed through a moving correlation analysis over 31 years (Figure 4d). From 1872 to 1917, there was a weak correlation between the iWUE and the $\delta^{18}\text{O}$, indicating that drought-induced effects were not necessary during this period, while from 1959 to 2018, there was no significant relationship between them, suggesting that other factors may have influenced the variations instead.

Water conditions, especially groundwater depth, influence *P. euphratica* growth, and soil organic matter content is one of its main determinants [66]. Zhang et al. [72] used stable isotope technology to explore water sources and utilization efficiency among different diameter classes of *P. euphratica* downstream of the Tarim River, concluding that water utilization efficiency would decrease with root growth at different stages. From 1958 to 2018, the BAI showed a “first increase then decrease” trend, while the iWUE continued to increase. This secondary relationship indicates that from 1958, when it was first cultivated, until 1982, when all indicators such as groundwater level and salinity, soil moisture content, and salt content were suitable for tree growth, trees utilized favorable conditions, resulting in a higher radial growth of *P. euphratica*. After 1983, under warm-humid climate conditions [73] and intensified background of human activities, over-matured *P. euphratica* entered a decline stage with an increased proportion of dead branches and roots [74], thus requiring an appropriate improvement in the iWUE to maintain their survival rather than promoting their growth during this period. Liu et al. [38] found that elevated atmospheric CO₂ concentrations significantly stimulated tree-ring width downstream of the Heihe River, Inner Mongolia, compensating for the negative impacts caused by the reduced river flow rate and drought during the study period. However, from 1850 to 1958, the BAI and iWUE may have been mainly affected by natural climatic factors, while from 1959 to 2018, human activities profoundly influenced them. The *P. euphratica* in the riparian forest has adapted to the increasing atmospheric CO₂ concentration, and has improved its water use efficiency and enhanced its growth ability. However, this adaptive capacity is unstable and easily affected by human activities.

The increase in atmospheric CO₂ concentrations promotes *P. euphratica* growth at a low frequency, but other factors (such as groundwater mineralization) may offset the potential benefits of rising carbon dioxide concentration [75]. Human activities have also promoted *P. euphratica* growth at a high frequency compared to historical periods.

5. Conclusions

This study conducted a comprehensive analysis using dendrochronology and isotope data ($\delta^{13}\text{C}$ and $\delta^{18}\text{O}$) to study the response of *P. euphratica* in the upstream region of Alaeer, Tarim Basin, to the increased atmospheric CO₂ concentration and human activities. From 1850 to 2018, we observed an increasing trend in the BAI and iWUE of *P. euphratica*, mainly due to the rising atmospheric CO₂ concentrations and favorable groundwater conditions. We found that 13% of this increase was attributed to changes in the water use efficiency (^{cc}iWUE) caused by elevated atmospheric CO₂ concentrations, a notably low value compared to non-riparian species. This limited response is likely due to the groundwater dependency of riparian species, which inherently limits their iWUE values and subsequent increases, resulting in less efficient water use. Around 1918, there was a shift from the weak correlation between the $\Delta^{13}\text{C}$ and $\delta^{18}\text{O}$ in tree rings, to a significant negative correlation, possibly related to the river channel migration upstream of the Tarim River. The BAI of *P. euphratica* growing along the Tarim River was positively correlated with the iWUE, indicating that an increased iWUE promoted tree growth somewhat. From 1958 to 1981, under human influence, *P. euphratica* grew rapidly. However, the iWUE continued to increase after 1983, and it did not promote further growth, as indicated by the secondary relationship between the BAI and iWUE, suggesting other factors, such as groundwater depth, were limiting growth. Overall, low-frequency increases in the atmospheric CO₂ concentrations promoted *P. euphratica* growth, while high-frequency increases were associated with human activities promoting its growth. Due to the lack of

long-term monitoring data on groundwater level fluctuations at this site, our interpretation needs further strengthening through future research.

Author Contributions: Conceptualization, methodology, software, and writing—original draft, Y.Y.; supervision, project administration, and funding acquisition, Y.L.; supervision, method, and editing, M.R. and Q.C.; chart drawing and data curation, C.S.; investigation and data curation, Q.L.; addition of the financing, H.S.; investigation, M.Y. and T.Z. All authors have read and agreed to the published version of the manuscript.

Funding: The study was financially supported by grants from the National Natural Science Foundation of China (U1803245), the second Tibetan Plateau Scientific Expedition and Research Program (STEP, 2019QZKK0101), the Strategic Priority Research Program of the Chinese Academy of Sciences (XDB40010300), and the China Desert Meteorological Science Research Foundation (SQJ2022012).

Data Availability Statement: Not applicable.

Conflicts of Interest: The authors declare no conflict of interest.

References

1. Anderegg, W.R.; Schwalm, C.; Biondi, F.; Camarero, J.J.; Koch, G.; Litvak, M.; Ogle, K.; Shaw, J.D.; Shevliakova, E.; Williams, A. Pervasive drought legacies in forest ecosystems and their implications for carbon cycle models. *Science* **2015**, *349*, 528–532. [[CrossRef](#)] [[PubMed](#)]
2. Carvalhais, N.; Forkel, M.; Khomik, M.; Bellarby, J.; Jung, M.; Migliavacca, M.; Saatchi, S.; Santoro, M.; Thurner, M.; Weber, U. Global covariation of carbon turnover times with climate in terrestrial ecosystems. *Nature* **2014**, *514*, 213–217. [[CrossRef](#)] [[PubMed](#)]
3. Wang, Y.; Tang, Y.; Xia, N.; Terrer, C.; Guo, H.; Du, E. Urban CO₂ imprints on carbon isotope and growth of Chinese pine in the Beijing metropolitan region. *Sci. Total Environ.* **2023**, *866*, 161389. [[CrossRef](#)]
4. Andreu-Hayles, L.; Planells, O.; Gutierrez, E.; Muntan, E.; Helle, G.; Anchukaitis, K.J.; Schleser, G.H. Long tree-ring chronologies reveal 20th century increases in water-use efficiency but no enhancement of tree growth at five Iberian pine forests. *Glob. Chang. Biol.* **2011**, *17*, 2095–2112. [[CrossRef](#)]
5. McCarroll, D.; Gagen, M.H.; Loader, N.J.; Robertson, I.; Anchukaitis, K.J.; Los, S.; Young, G.H.F.; Jalkanen, R.; Kirchhefer, A.; Waterhouse, J.S. Correction of tree ring stable carbon isotope chronologies for changes in the carbon dioxide content of the atmosphere. *Geochim. Cosmochim. Acta* **2009**, *73*, 1539–1547. [[CrossRef](#)]
6. Liu, Y.; Song, H.; An, Z.; Sun, C.; Zeng, X. Recent anthropogenic curtailing of Yellow River runoff and sediment load is unprecedented over the past 500 y. *Proc. Natl. Acad. Sci. USA* **2020**, *117*, 201922349.
7. Fritts, H. *Tree Rings and Climate*; Academic Press: New York, NY, USA, 2012; p. 567.
8. Yu, P.; Xu, H.; Ye, M.; Liu, S.; Gong, J.; An, H.; Fu, J. Effects of ecological water conveyance on the ring increments of *Populus euphratica* in the lower reaches of Tarim River. *J. For. Res.* **2012**, *17*, 413–420. [[CrossRef](#)]
9. Farquhar, G.; O’Leary, M.; Berry, J. On the relationship between carbon isotope discrimination and the intercellular carbon dioxide concentration in Leaves. *Funct. Plant Biol.* **1982**, *9*, 121–137. [[CrossRef](#)]
10. McCarroll, D.; Loader, N.J. Stable isotopes in tree rings. *Quat. Sci. Rev.* **2004**, *23*, 771–801. [[CrossRef](#)]
11. Scheidegger, Y.; Saurer, M.; Bahn, M.; Siegwolf, R. Linking stable oxygen and carbon isotopes with stomatal conductance and photosynthetic capacity: A conceptual model. *Oecologia* **2000**, *125*, 350–357. [[CrossRef](#)]
12. Castruita-Esparza, L.U.; Silva, L.C.R.; Gomez-Guerrero, A.; Villanueva-Diaz, J.; Correa-Diaz, A.; Horwath, W.R. Coping with extreme events: Growth and Water-Use Efficiency of trees in Western Mexico during the driest and wettest periods of the past one hundred sixty years. *J. Geophys. Res. Biogeosci.* **2019**, *124*, 3419–3431. [[CrossRef](#)]
13. Mathias, J.M.; Thomas, R.B. Global tree intrinsic water use efficiency is enhanced by increased atmospheric CO₂ and modulated by climate and plant functional types. *Proc. Natl. Acad. Sci. USA* **2021**, *118*, e2014286118. [[CrossRef](#)] [[PubMed](#)]
14. Lu, W.W.; Yu, X.X.; Jia, G.D.; Li, H.Z.; Liu, Z.Q. Responses of intrinsic water-use efficiency and tree growth to climate change in semi-arid areas of North China. *Sci. Rep.* **2018**, *8*, 308.
15. Peng, Z.; Zhang, Y.; Zhu, L.; Guo, M.; Lu, Q.; Xu, K.; Shao, H.; Mo, Q.; Liu, S. Spatial and temporal patterns of the sensitivity of radial growth response by *Picea schrenkiana* to regional climate change in the Tianshan Mountains. *J. For. Res.* **2023**, 1–13. [[CrossRef](#)]
16. Wang, Y.; Zhang, Y.; Fang, O.Y.; Shao, X.M. Long-term changes in the tree radial growth and intrinsic water-use efficiency of Chuanxi spruce (*Picea likiangensis* var. *balfouriana*) in southwestern China. *J. Geogr. Sci.* **2018**, *28*, 833–844.
17. Huang, R.; Zhu, H.; Liu, X.; Liang, E.; Grießinger, J.; Wu, G.; Li, X.; Bräuning, A. Does increasing intrinsic water use efficiency (iWUE) stimulate tree growth at natural alpine timberline on the southeastern Tibetan Plateau? *Glob. Planet. Chang.* **2017**, *148*, 217–226. [[CrossRef](#)]
18. Jia, G.D.; Chen, L.X.; Yu, X.X.; Liu, Z.Q. Soil water stress overrides the benefit of water-use efficiency from rising CO₂ and temperature in a cold semi-arid poplar plantation. *Plant Cell Environ.* **2022**, *45*, 1172–1186. [[CrossRef](#)]

19. Chen, Z.C.; Zhang, Y.D.; Li, Z.S.; Han, S.J.; Wang, X.C. Climate change increased the intrinsic water use efficiency of *Larix gmelinii* in permafrost degradation areas, but did not promote its growth. *Agric. For. Meteorol.* **2022**, *320*, 108957. [[CrossRef](#)]
20. LaMarche, V.C.; Graybill, D.A.; Fritts, H.C.; Rose, M.R. Increasing atmospheric carbon dioxide: Tree ring evidence for growth enhancement in natural vegetation. *Science* **1984**, *225*, 1019–1021. [[CrossRef](#)]
21. Schook, D.M.; Friedman, J.M.; Stricker, C.A.; Csank, A.Z.; Cooper, D.J. Short- and long-term responses of riparian cottonwoods (*Populus* spp.) to flow diversion: Analysis of tree -ring radial growth and stable carbon isotopes. *Sci. Total Environ.* **2020**, *735*, 139523. [[CrossRef](#)]
22. Kannenberg, S.A.; Driscoll, A.W.; Szejner, P.; Anderegg, W.R.L.; Ehleringer, J.R. Rapid increases in shrubland and forest intrinsic water-use efficiency during an ongoing megadrought. *Proc. Natl. Acad. Sci. USA* **2021**, *118*, e2118052118. [[CrossRef](#)] [[PubMed](#)]
23. Yin, T.T.; Zhai, Y.N.; Zhang, Y.; Yang, W.J.; Dong, J.B.; Liu, X.; Fan, P.X.; You, C.; Yu, L.Q.; Gao, Q.; et al. Impacts of climate change and human activities on vegetation coverage variation in mountainous and hilly areas in Central South of Shandong Province based on tree-ring. *Front Plant Sci* **2023**, *14*, 1158221. [[CrossRef](#)] [[PubMed](#)]
24. Albiero, A.; Camargo, J.L.C.; Roig, F.A.; Schongart, J.; Pinto, R.M.; Venegas-Gonzalez, A.; Tomazello-Filho, M. Amazonian trees show increased edge effects due to Atlantic Ocean warming and northward displacement of the Intertropical Convergence Zone since 1980. *Sci. Total Environ.* **2019**, *693*, 133515. [[CrossRef](#)] [[PubMed](#)]
25. Dangerfield, C.R.; Voelker, S.L.; Lee, C.A. Long-term impacts of road disturbance on old-growth coast redwood forests. *For. Ecol. Manag.* **2021**, *499*, 119595. [[CrossRef](#)]
26. Sensula, B.M. $\delta^{13}\text{C}$ and Water Use Efficiency in the Glucose of annual pine tree rings as ecological indicators of the forests in the most industrialized part of Poland. *Water Air Soil Poll.* **2016**, *227*, 68. [[CrossRef](#)]
27. Guerrieri, R.; Vanguelova, E.; Pitman, R.; Benham, S.; Perks, M.; Morison, J.I.L.; Mencuccini, M. Climate and atmospheric deposition effects on forest water-use efficiency and nitrogen availability across Britain. *Sci. Rep.* **2020**, *10*, 12418. [[CrossRef](#)]
28. Liu, W.F.; Duan, H.L.; Shen, F.F.; Liao, Y.C.; Li, Q.; Wu, J.P. Effects of long-term nitrogen addition on water use by Cunninghamia lanceolata in a subtropical plantation. *Ecosphere* **2022**, *13*, e4033. [[CrossRef](#)]
29. Sensula, B.M. Spatial and Short-Temporal variability of $\delta^{13}\text{C}$ and $\delta^{15}\text{N}$ and water-use efficiency in pine needles of the three forests along the most industrialized part of Poland. *Water Air Soil Poll.* **2015**, *226*, 362.1. [[CrossRef](#)]
30. Krause, K.; Cherubini, P.; Bugmann, H.; Schleppi, P. Growth enhancement of *Picea abies* trees under long-term, low-dose N addition is due to morphological more than to physiological changes. *Tree Physiol.* **2012**, *32*, 1471–1481. [[CrossRef](#)]
31. Bachar, A.; Markus-Shi, J.; Regev, L.; Boaretto, E.; Klein, T. Tree rings reveal the adverse effect of water pumping on protected riparian *Platanus orientalis* tree growth. *For. Ecol. Manag.* **2020**, *458*, 117784. [[CrossRef](#)]
32. Matulewski, P.; Buchwal, A.; Makohonienko, M. Higher climatic sensitivity of Scots pine (*Pinus sylvestris* L.) subjected to tourist pressure on a hiking trail in the Brodnica Lakeland, NE Poland. *Dendrochronologia* **2019**, *54*, 78–86. [[CrossRef](#)]
33. Zhou, T.H.; Zhao, C.Y.; Wu, G.L.; Jiang, S.W.; Yu, Y.X.; Wang, D.D. Application of stable isotopes in analyzing the water sources of *Populus euphratica* and *Tamarix ramosissima* in the upstream of Tarim River. *J. Desert Res.* **2017**, *37*, 124–131. (In Chinese)
34. Zhou, H.H.; Chen, Y.N.; Zhu, C.G.; Li, Z.; Fang, G.H.; Li, Y.P.; Fu, A.H. Climate change may accelerate the decline of desert riparian forest in the lower Tarim River, Northwestern China: Evidence from tree-rings of *Populus euphratica*. *Ecol. Indic.* **2020**, *111*, 105997. [[CrossRef](#)]
35. Lang, P.; Ahlborn, J.; Schaefer, P.; Wommelsdorf, T.; Jeschke, M.; Zhang, X.M.; Thomas, F.M. Growth and water use of *Populus euphratica* trees and stands with different water supply along the Tarim River, N.W. China. *For. Ecol. Manag.* **2016**, *380*, 139–148. [[CrossRef](#)]
36. Ling, H.; Guo, B.; Zhang, G.; Xu, H.; Deng, X. Evaluation of the ecological protective effect of the "large basin" comprehensive management system in the Tarim River basin, China. *Sci. Total Environ.* **2019**, *650*, 1696–1706. [[CrossRef](#)] [[PubMed](#)]
37. Deng, X.Y.; Xu, H.L.; Ye, M.; Li, B.L.; Fu, J.Y.; Yang, Z.F. Impact of long-term zero-flow and ecological water conveyance on the radial increment of *Populus euphratica* in the lower reaches of the Tarim River, Xinjiang, China. *Reg. Environ. Chang.* **2015**, *15*, 13–23. [[CrossRef](#)]
38. Liu, X.H.; Wang, W.Z.; Xu, G.B.; Zeng, X.M.; Wu, G.J.; Zhang, X.W.; Qin, D.H. Tree growth and intrinsic water-use efficiency of inland riparian forests in northwestern China: Evaluation via delta C-13 and delta O-18 analysis of tree rings. *Tree Physiol.* **2014**, *34*, 966–980. [[CrossRef](#)]
39. The Fourteenth Xinjiang Production and Construction Corps History Compilation Committee Division. *The Local Chronicles of the Fourteenth Division of Xinjiang Production and Construction Corps*; Xinjiang People's Publishing House: Urumqi, China, 2000; p. 20. (In Chinese)
40. Holmes, R.L. Computer-assisted quality control in tree-ring dating and measurement. *Tree-Ring Bull.* **1983**, *43*, 69–78.
41. Bunn, A.G. A dendrochronology program library in R (dplR). *Dendrochronologia* **2008**, *26*, 115–124. [[CrossRef](#)]
42. Biondi, F.; Qeadan, F. A theory-driven approach to tree-ring standardization: Defining the biological trend from expected basal area increment. *Tree-Ring Res.* **2008**, *64*, 81–96. [[CrossRef](#)]
43. Liu, Y.; Ren, M.; Li, Q.; Song, H.; Liu, R. Tree-ring $\delta^{18}\text{O}$ based July-August relative humidity reconstruction on Mt. Shimen, China, for the last 400 years. *Atmos. Res.* **2020**, *243*, 105024. [[CrossRef](#)]
44. Liu, Y.; Wang, L.; Li, Q.; Cai, Q.F.; Song, H.M.; Sun, C.F.; Liu, R.S.; Mei, R.C. Asian summer monsoon-related relative humidity recorded by tree ring $\delta^{18}\text{O}$ during last 205 Years. *J. Geophys. Res. -Atmos.* **2019**, *124*, 9824–9838. [[CrossRef](#)]

45. Coplen, T.B.; Brand, W.A.; Gehre, M.; Gröning, M.; Meijer, H.A.; Toman, B.; Verkouteren, R.M. New guidelines for $\delta^{13}\text{C}$ measurements. *Anal. Chem.* **2006**, *78*, 2439–2441. [\[CrossRef\]](#) [\[PubMed\]](#)
46. Saugier, B.; Ehleringer, J.R.; Hall, A.E.; Farquhar, G.D. *Stable isotopes and plant carbon-water relations*; Academic Press: San Diego, CA, USA, 1993; p. 463.
47. Frank, D.C.; Poulter, B.; Saurer, M.; Esper, J.; Huntingford, C.; Helle, G.; Treydte, K.; Zimmermann, N.E.; Schleser, G.H.; Ahlstrom, A.; et al. Water-use efficiency and transpiration across European forests during the Anthropocene. *Nat. Clim. Chang.* **2015**, *5*, 579. [\[CrossRef\]](#)
48. Pachauri, R.K.; Allen, M.R.; Barros, V.R.; Broome, J.; Cramer, W.; Christ, R.; Church, J.A.; Clarke, L.; Dahe, Q.; Dasgupta, P.; et al. *Climate Change 2014: Synthesis Report. Contribution of Working Groups I, II and III to the Fifth Assessment Report of the Intergovernmental Panel on Climate Change*; IPCC: Geneva, Switzerland, 2014; p. 151.
49. Saurer, M.; Siegwolf, R.T.W.; Schweingruber, F.H. Carbon isotope discrimination indicates improving water-use efficiency of trees in northern Eurasia over the last 100 years. *Glob. Chang. Biol.* **2004**, *10*, 2109–2120. [\[CrossRef\]](#)
50. Adams, M.A.; Buckley, T.N.; Turnbull, T.L. Diminishing CO₂-driven gains in water-use efficiency of global forests. *Nat. Clim. Chang.* **2020**, *10*, 466–471. [\[CrossRef\]](#)
51. Zhao, C.Y. Water Use Strategies and Adaptation to Drought Stress in *Populus euphratica* of Riparian Desert Forest. Doctor's Thesis, University of Chinese Academy of Sciences, Beijing, China, 2019. (In Chinese).
52. Hetherington, A.M.; Woodward, F.I. The role of stomata in sensing and driving environmental change. *Nature* **2003**, *424*, 901–908. [\[CrossRef\]](#)
53. Grossiord, C.; Buckley, T.N.; Cernusak, L.A.; Novick, K.A.; Poulter, B.; Siegwolf, R.T.; Sperry, J.S.; McDowell, N.G. Plant responses to rising vapour pressure deficit. *New Phytol.* **2020**, *226*, 1550–1566. [\[CrossRef\]](#)
54. Liu, X.H.; Xu, G.B.; Wang, W.Z.; Wu, G.J.; Zeng, X.M.; An, W.L.; Zhang, X.W. Tree-ring stable isotopes proxies: Progress, problems and prospects. *Quat. Sci.* **2015**, *35*, 1245–1260. (In Chinese)
55. Han, C.X. Channel change of Tarim River and its response to human activities from the 18th century. *J. Desert Res.* **2011**, *31*, 1072–1078. (In Chinese)
56. Yu, G.A.; Li, Z.W.; Huang, H.Q.; Liu, X.F. Human impacts on fluvial processes in a very arid environment: The case of Tarim River in China. *Adv. Water Sci.* **2017**, *28*, 183–192. (In Chinese)
57. Li, X.; Nian, F.H. Effect of human activities on groundwater in Alaer irrigation area in Xinjiang. *J. Arid Land Resour. Environ.* **1999**, *13*, 41–47. (In Chinese)
58. Yong, Z.; Zhao, C.Y.; Shi, F.Z.; Ma, X.F. Variation characteristics of groundwater depth and its ecological effect in the mainstream of Tarim River in recent 20 years. *J. Soil Water Conserv.* **2020**, *34*, 182–189.
59. Peng, X.M.; Xiao, S.C.; Cheng, G.D.; Xiao, H.L.; Tian, Q.Y.; Zhang, Q.B. Human activity impacts on the stem radial growth of *Populus euphratica* riparian forests in China's Ejina Oasis, using tree-ring analysis. *Trees-Struct. Funct.* **2017**, *31*, 379–392. [\[CrossRef\]](#)
60. Si, J.; Feng, Q.; Cao, S.; Yu, T.; Zhao, C. Water use sources of desert riparian *Populus euphratica* forests. *Env. Monit Assess* **2014**, *186*, 5469–5477. [\[CrossRef\]](#)
61. Zhou, M.X.; Xiao, H.L.; Luo, F.; Li, S.Z.; Song, Y.X.; Xiao, C.S. Groundwater salinity characters and their relationship with vegetation growth in Ejin delta. *J. Desert Res.* **2004**, *24*, 6. (In Chinese)
62. Li, J.F. The yearly ring and water-heat index in the middle reach of the Tarim River. *Arid Land Geogr.* **1988**, *11*, 17–23. (In Chinese)
63. Li, J.F.; Yuan, Y.J.; You, X.Y. *Research and Application of Tree Ring Hydrology*; Science Press: Beijing, China, 2000; pp. 22–23. (In Chinese)
64. Zheng, D.; Li, W.H.; Chen, Y.P.; Liu, J.Z. Relations between groundwater and natural vegetation in the arid zone. *Resour. Sci.* **2005**, *27*, 160–167. (In Chinese)
65. Wang, J. Study on the relationship between vegetation and brackish water distribution in Alar Oasis. Master's Thesis, Shihezi University, Shihezi, China, 2019. (In Chinese).
66. Huo, A.; Wang, X.; Guan, W.; Zhong, J.; Yi, X.; Wen, Y. Soil physico-chemical properties and their effects on *Populus euphratica* growth in desertification areas. *Ukr. J. Ecol.* **2019**, *9*, 21–27.
67. Franks, P.J.; Adams, M.A.; Amthor, J.S.; Barbour, M.M.; Berry, J.A. Sensitivity of plants to changing atmospheric CO₂ concentration: From the geological past to the next century. *New Phytol.* **2013**, *197*, 1077–1094. [\[CrossRef\]](#)
68. Rahman, M.; Islam, M.; Gebrekirstos, A.; Bräuning, A. Disentangling the effects of atmospheric CO₂ and climate on intrinsic water-use efficiency in South Asian tropical moist forest trees. *Tree Physiol.* **2020**, *40*, 904–916. [\[CrossRef\]](#)
69. Chen, Y.; Chen, Y.; Xu, C.; Li, W. Groundwater depth affects the daily course of gas exchange parameters of *Populus euphratica* in arid areas. *Environ. Earth Sci.* **2012**, *66*, 433–440. [\[CrossRef\]](#)
70. Zhang, Q.; Ficklin, D.L.; Manzoni, S.; Wang, L.; Way, D.; Phillips, R.P.; Novick, K.A. Response of ecosystem intrinsic water use efficiency and gross primary productivity to rising vapour pressure deficit. *Environ. Res. Lett.* **2019**, *14*, 074023. [\[CrossRef\]](#)
71. Yuan, W.; Zheng, Y.; Piao, S.; Ciais, P.; Lombardozzi, D.; Wang, Y.; Ryu, Y.; Chen, G.; Dong, W.; Hu, Z. Increased atmospheric vapour pressure deficit reduces global vegetation growth. *Sci. Adv.* **2019**, *5*, eaax1396. [\[CrossRef\]](#) [\[PubMed\]](#)
72. Zhang, J.; Li, G.F.; He, Y.L.; Mu, Y.D.; Zhuang, L.; Liu, H.L. Water utilization sources of *Populus euphratica* trees of different ages in the lower reaches of Tarim River. *Biodivers. Sci.* **2018**, *26*, 564–571. (In Chinese) [\[CrossRef\]](#)

73. Shi, Y.F.; Shen, Y.P.; Li, D.L.; Zhang, G.W.; Ding, Y.J.; Hu, R.J.; Kang, E.S. Discussion on the present climate change from Warm-dry to Warm-wet in Northwest China. *Quat. Sci.* **2003**, *23*, 152–164. (In Chinese)
74. Yuan, Y.P.; Zhao, Y.; Zhao, C.Y.; Li, W.J. Characteristics of the foliar stable carbon isotope composition of *Populus euphratica* for different Niche in the Lower Reach of the Heihe River. *J. Desert Res.* **2015**, *35*, 1505–1511. (In Chinese)
75. Silva, L.C.R.; Anand, M. Probing for the influence of atmospheric CO₂ and climate change on forest ecosystems across biomes probing for the influence of atmospheric CO₂ and climate change on forest ecosystems across biomes. *Glob. Ecol. Biogeogr.* **2013**, *22*, 83–92. [[CrossRef](#)]

Disclaimer/Publisher’s Note: The statements, opinions and data contained in all publications are solely those of the individual author(s) and contributor(s) and not of MDPI and/or the editor(s). MDPI and/or the editor(s) disclaim responsibility for any injury to people or property resulting from any ideas, methods, instructions or products referred to in the content.